PROJECT REPORT

On

"DESIGN, SYNTHESIS, CHARACTERIZATION, AND ANTIBACTERIAL ACTIVITY OF NOVEL QUERCETIN SCHIFF BASE DERIVATIVES"

Submitted by

BLESSY P.L. (AB23CHE019)

In partial fulfilment for the award of the

Bachelor's Degree in Chemistry

DEPARTMENT OF CHEMISTRY AND CENTRE FOR RESEARCH

ST. TERESA'S COLLEGE (AUTONOMOUS)
ERNAKULAM

2025-2026

DEPARTMENT OF CHEMISTRY AND CENTRE FOR RESEARCH

ST. TERESA'S COLLEGE (AUTONOMOUS)

ERNAKULAM

B.Sc. CHEMISTRY PROJECT REPORT

Name : BLESSY P.L.
Register Number: AB23CHE019
Year of Work : 2025-2026

This is to certify that the project **"DESIGN, SYNTHESIS, CHARACTERIZATION, AND ANTIBACTERIAL ACTIVITY OF NOVEL QUERCETIN SCHIFF BASE DERIVATIVES"** is the work done by **BLESSY P.L.**

Dr. Saritha Chandran A.
Head of the Department

Dr.Shanty A.A.
Staff-member in charge

Submitted to the Examination of Bachelor's Degree in Chemistry

Date: 03/04/2026

Examiners: .....

DEPARTMENT OF CHEMISTRY AND CENTRE FOR RESEARCH

ST. TERESA'S COLLEGE (AUTONOMOUS)

ERNAKULAM

CERTIFICATE

This is to certify that the project work entitled **"DESIGN, SYNTHESIS, CHARACTERIZATION, AND ANTIBACTERIAL ACTIVITY OF NOVEL QUERCETIN SCHIFF BASE DERIVATIVES" is** the work done by **BLESSY P.L.** under my guidance in the partial fulfilment of the award of the Degree of Bachelor of Science in Chemistry at St. Teresa's College (Autonomous), Ernakulam affiliated to Mahatma Gandhi University, Kottayam.

Dr.Shanty A.A.

Project Guide

DECLARATION

I hereby declare that the project work entitled **"DESIGN, SYNTHESIS, CHARACTERIZATION, AND ANTIBACTERIAL ACTIVITY OF NOVEL QUERCETIN SCHIFF BASE DERIVATIVES"** submitted to Department of Chemistry and Centre for Research, St. Teresa's College (Autonomous) affiliated to Mahatma Gandhi University, Kottayam, is a record of an original work done by me under the guidance of **Dr.Shanty A.A.,** Department of Chemistry and Centre for Research, St. Teresa's College (Autonomous), Ernakulam and this project work is submitted in the partial fulfilment of the requirements for the award of the Degree of Bachelor of Science in Chemistry.

Blessy

BLESSY P.L.

Acknowledgements

With deep appreciation, we wish to thank the Almighty for His constant blessings, guidance, and strength which enabled us to complete this project successfully.

We express our sincere and heartfelt gratitude to our guide, Dr.Shanty A.A., Assistant Professor, Department of Chemistry, for her constant guidance, valuable suggestions, encouragement, and unwavering support throughout the course of this project. Her mentorship has been instrumental in the successful completion of this work.

We also extend our sincere gratitude to Dr.Saritha Chandran A., Head of the Department of Chemistry, for her encouragement and support.

We take this opportunity to express our sincere thanks to Dr.Anu Joseph, Principal; Rev. Sr. Nilima CSST, Manager; and the Directors, Rev. Sr. Francis Ann CSST and Rev. Sr. Tessa CSST, St. Teresa's College (Autonomous), Ernakulam, for being the pillars of support and for providing excellent infrastructure and a conducive academic environment for research and learning.

We express our heartfelt thanks to all the faculty members of the Department of Chemistry and the Centre for Research for their wholehearted support, guidance, and encouragement. We also sincerely thank the non-teaching staff and laboratory faculties for their technical

assistance and continuous support throughout the execution of this project.

We gratefully acknowledge TICC, St. Teresa's College (Autonomous), Ernakulam; the Sophisticated Test and Instrumentation Centre (SAIF), Cochin University of Science and Technology (CUSAT), Kochi, India; and the Instrumentation Facility at Bharat Mata College, for providing the necessary instrumental facilities and technical support required for the successful completion of this work.

Finally, we heartily thank our family and friends for their constant encouragement, moral support, and motivation which helped us accomplish this project successfully.

Blessy

BLESSY P. L.

Contents

Chapter 1

Introduction

1.1 QUERCETIN

Quercetin (2-(3′,4′-dihydroxyphenyl)-3,5,7-trihydroxychromen-4-one) is a naturally occurring flavonol found widely in fruits, vegetables, and beverages, consisting of two benzene rings linked by a heterocyclic pyrone ring with five hydroxyl groups *(Figure1.1)*, responsible for its biological activity, and its name derives from the Latin *quercetum* ("oak forest") [1], it is a yellow crystalline solid with a bitter taste, insoluble in water, partially soluble in alcohol and lipids, soluble in alkaline solutions, and has a molecular formula of $C_{15}H_{10}O_7$ with a molecular mass of 302.236 g/mol.

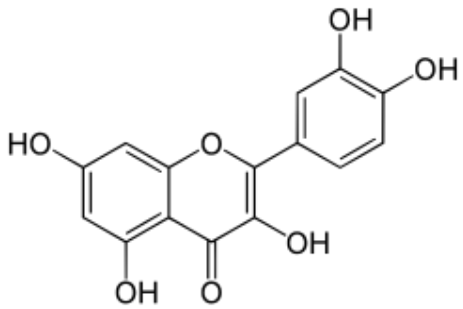

Figure1.1: 2-(3,4-dihydroxyphenyl)-3,5,7-trihydroxychromen-4-one

Quercetin is absorbed in the intestine and metabolized in the liver, where it exerts cardioprotective, anticancer, and neuroprotective effects through antioxidant, anti-inflammatory, and gene-regulating mechanisms, making it a promising lead compound for developing more potent therapeutic derivatives [2], and as a plant-derived polyphenol, it functions as a potent

free radical scavenger that inhibits lipid peroxidation and protects cells from oxidative stress, with bioavailability influenced by absorption, metabolism, and glycoside conversion, while substantial evidence supports the protective role of quercetin-rich foods against chronic and degenerative diseases [3], justifying the development of quercetin-based Schiff base derivatives to enhance antibacterial and therapeutic efficacy.

1.2 BIOLOGICAL PROPERTIES OF QUERCETIN

1.2.1 Antioxidant Property

Quercetin is a potent antioxidant that scavenges free radicals, chelates transition metals, inhibits lipid peroxidation, reduces oxidative stress linked to cardiovascular and neurodegenerative diseases, and exerts anti-inflammatory effects by blocking pro-inflammatory cytokine activation, with its activity depending on hydrogen donation and neutralization of ROS and RNS, although, as noted by Pietta et al.,[4] correlating its structure with radical-scavenging efficiency remains complex; its antioxidant efficiency is influenced by chemical structure—particularly the 3′-OH and 4′-OH groups in the B-ring—which enhance radical-scavenging activity, promote metal ion binding, lower bond dissociation energy, and increase the antioxidant potential of quercetin and its complexes, including quercetin–DNA interactions [5].

Although quercetin exhibits strong antioxidant activity in vitro, its in vivo effects are limited by absorption, metabolism, and bioavailability, producing various metabolites and only modest increases in plasma antioxidant capacity [6], while its antioxidant activity is dynamic and influenced by environmental factors like solvent and temperature, with antiradical activity sometimes initially increasing during degradation

before declining due to oxidative reactions, reflecting the combined impact of its structure and external conditions [7].

1.2.2 Anti Inflammatory Property

Quercetin and its derivatives exhibit significant anti-inflammatory activity by inhibiting mediators such as 12-HHT, TXB_2, PGE_2, and 12-HETE in a concentration-dependent manner comparable to aspirin, with circulating metabolites including those from dietary sources like Allium cepa (onion) contributing substantially to their antioxidant and anti-inflammatory effects [8], while in vivo studies, such as those by Lin et al., show it reduces inflammatory responses like paw edema in rats, with effectiveness dependent on formulation and bioavailability, as better-absorbed derivatives demonstrate stronger effects [9].

Quercetin demonstrates anti-inflammatory effects in conditions like atopic dermatitis by modulating immune responses, inhibiting mediators such as IL-6, IL-8, TNF-α, histamine, and tryptase, and suppressing multiple inflammatory pathways, making it a promising plant-based alternative to long-term steroid therapy [10], while in cardiovascular disease models, it reduces inflammatory markers, suppresses vascular inflammation, and attenuates atherosclerosis-related signalling, with long-term supplementation linked to decreased lesion formation and enhanced cardioprotective potential [11].

1.2.3 Anti-Cancer Property

Quercetin is a naturally occurring flavonoid recognized for its significant anticancer potential, acting as a chemo preventive agent by inhibiting cancer cell proliferation and angiogenesis, inducing apoptosis, cellular senescence, and cell cycle arrest, with cell culture studies showing slowed

cancer growth and promoted apoptosis, animal studies indicating protective effects particularly against colon cancer [12] and clinical studies, such as those by Cruz-Correa et al., demonstrating that quercetin combined with curcumin significantly reduced the number and size of ileal and rectal adenomas in FAP patients with minimal side effects, highlighting its therapeutic potential in cancer management [13].

It acts as a chemo preventive agent by inhibiting cancer cell growth and progression, suppressing proliferation, and promoting apoptosis in various cancer cell lines [14], at low concentrations it functions as an antioxidant, while at higher doses it may exhibit pro-oxidant activity that increases oxidative stress in cancer cells and inhibits tumor growth, with animal studies supporting its protective role particularly in colon and breast cancers and its interference with key signaling pathways involved in cancer progression, inflammation, and angiogenesis [15], while at 26.5–50 μM it reduces glucose and lactate production in breast cancer and tumor cells, indicating inhibition of glycolysis, a key metabolic pathway in cancer [16], and its natural origin, wide availability, broad biological activity, and relatively low toxicity make it a promising, safe, and cost-effective complementary agent for cancer prevention and therapy , used alone or alongside chemotherapeutic drugs, though further research is needed [17].

1.2.4 Neurological Effects

Quercetin exhibits both neuroprotective and neurotoxic effects depending on dose, exposure time, and cellular redox balance, with studies showing its neuroprotective potential. Joseph et al. reported that combined administration with fish oil protected the rat brain and showed benefits against neurodegenerative disorders like Alzheimer’s disease, while it also

inhibits acetylcholinesterase activity, a key target in cognitive decline [18].

Extensive in vitro, animal, and clinical studies demonstrate that quercetin provides neuroprotection against neuronal injury and neurotoxicity, showing benefits in neurodegenerative disorders such as Alzheimer's, Parkinson's, Huntington's, multiple sclerosis, amyotrophic lateral sclerosis, and amyloid-β-associated neurodegeneration through its antioxidant, anti-inflammatory, anti-apoptotic properties, and regulation of neuronal survival pathways [19], while recent studies also highlight its antiepileptic potential by modulating neurotransmitter systems, electrical activity, and ion channels to reduce seizure frequency involved in epilepsy. Through its multi-target actions on neural cells and signaling pathways, quercetin contributes to neuroprotection in epileptic conditions [20].

1.2.5 Antiviral Property

Quercetin exhibits notable antiviral activity, particularly against enveloped viruses such as herpes simplex type I, parainfluenza type 3, respiratory syncytial virus, pseudorabies virus, Sindbis virus, and cardio viruses, by binding viral coat proteins and polymerases, interfering with replication, modulating DNA integrity, and enhancing the activity of antiviral agents like interferon [21], recent in silico and in vitro studies also show it disrupts multiple stages of viral entry and replication, including inhibition of SARS-CoV-2 enzymes (PLpro, 3CLpro, NTPase/helicase) and suppression of NLRP3 inflammasome activation, reducing proinflammatory cytokines linked to severe respiratory damage [22].

1.2.6 Anti-Microbial Property

Quercetin shows antibacterial activity against pathogens affecting the gastrointestinal, respiratory, urinary, and skin systems. Its efficacy depends on its solubility and interaction with bacterial membranes, influenced by hydroxyl groups. Gram-negative bacteria are generally more resistant than Gram-positive bacteria, though certain derivatives demonstrate improved activity against Gram-negative strains. Structural modifications such as phosphorylation or sulfation can further alter its antibacterial potential. It has shown inhibitory effects against organisms such as *Streptococcus mutans, Staphylococcus aureus, Pseudomonas aeruginosa, Shigella sonnei,* and methicillin-resistant *S. aureus*. Quercetin also acts synergistically with antibiotics and other agents, enhancing antibacterial efficacy against resistant strains [23].

Quercetin exhibits broad-spectrum antimicrobial activity through multiple mechanisms, including increasing bacterial cell permeability, disrupting cell walls, inhibiting nucleic acid and protein synthesis, and reducing enzyme activity, showing strong inhibitory effects against bacteria and fungi such as *Salmonella enterica*, *Escherichia coli*, *Pseudomonas aeruginosa*, *Staphylococcus aureus*, and *Aspergillus* [24], certain isatin- and isoniazid-derived Schiff bases demonstrate high potency, selectivity, and low cytotoxicity, highlighting their potential as antitubercular agents against *Mycobacterium tuberculosis* [25], while quercetin's incorporation into bio-based food packaging enhances antimicrobial functionality, thereby improving food safety and extending product shelf life [26], and its activity varies with microorganism type and concentration, showing synergistic effects with other antimicrobials, supporting its role as a lead

compound for developing structurally modified derivatives with improved antibacterial activity.

1.3 SCHIFF BASE

The term Schiff base was introduced by the German chemist Hugo Schiff in 1864 during his studies on the reaction between primary amines and carbonyl compounds. According to IUPAC, Schiff bases are imine compounds with the general formula $R_2C = NR'$ *(Figure1.2)* and are also known as azomethines due to the presence of the characteristic –C=N– group [27].

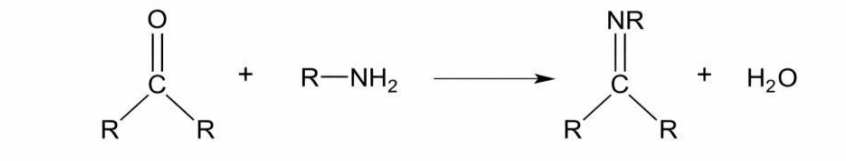

Figure1.2: Condensation reaction of amines with aldehyde or ketone to form Schiff base

Schiff bases are widely used in industry as dyes, pigments, catalysts, polymer stabilizers, and synthetic intermediates. They also exhibit a broad spectrum of biological activities, including antibacterial, antifungal, antiviral, antimalarial, anti-inflammatory, and antiproliferative effects, with the imine (–C=N–) group playing a crucial role in their activity, making them important scaffolds in medicinal chemistry [28]. Their biological activity is often enhanced upon complexation with transition metals, contributing significantly to coordination chemistry, inorganic biochemistry, and functional materials. Additionally, Schiff bases serve as versatile synthons for synthesizing various industrially and biologically active heterocyclic compounds, encouraging the design of novel derivatives for advanced and environmentally friendly applications [29].

1.3.1 Applications of Schiff Base Compound

Schiff bases and their metal complexes are versatile compounds with significant biological, catalytic, and industrial applications, as their ability to coordinate with p- and d-block metals allows modification of steric and electronic properties, enhancing reactivity and selectivity; many transition metal–Schiff base complexes serve as efficient catalysts in oxidation, hydrogenation, polymerization, and asymmetric synthesis, while biologically, certain Schiff bases such as thiosemicarbazones exhibit strong antiproliferative activity, and their metal complexes especially with iron and copper, enhance activity by inhibiting ribonucleotide reductase, inducing cell cycle arrest and apoptosis [30].

Advances in bioinorganic chemistry further highlight Schiff base metal complexes as promising antimicrobial agents, with complexes of Fe(III), Co(II), Ni(II), UO_2(II), and Pt(II) showing superior antibacterial activity compared to free ligands against pathogens including *Escherichia coli*, *Pseudomonas aeruginosa*, *Staphylococcus aureus*, *Staphylococcus pyogenes*, and *Bacillus subtilis*, largely due to increased lipophilicity that enhances membrane penetration [31].

Due to their simple synthesis and strong metal-chelating ability, Schiff bases exhibit diverse biological activities and are widely used as optical and electrochemical chemo sensors for detecting metal ions in environmental and biological systems, offering a more cost-effective, sensitive, and rapid alternative to conventional methods, with selectivity determined by metal ion size, charge, and coordination properties, enabling efficient colorimetric or fluorescent “turn-on/turn-off” detection of toxic and environmentally relevant ions [32]. Overall, Schiff bases and their metal complexes constitute a versatile class of compounds with

broad applications in catalysis, sensing, materials science, and medicinal chemistry, and their structural flexibility and strong coordination properties continue to drive significant research interest.

1.3.2 Biological Activities of Quercetin-Based Schiff Bases

Figure1.3: Biological applications of Schiff bases

1.4 BACTERIA USED FOR STUDY

1.4.1 *Bacillus cereus*

Bacillus cereus is a Gram-positive, spore-forming bacterium *(Figure1.4.1)* belonging to the *B. cereus* group, commonly associated with food poisoning, particularly from rice-based dishes. During growth, it produces enzymes and toxins such as phospholipases, proteases, hemolysins, and cereolysin, contributing to non-gastrointestinal infections. Once

considered a contaminant, *B. cereus* is now recognized as a cause of serious infections including endophthalmitis, septicemia, meningitis, endocarditis, and wound infections, especially in immunocompromised and postsurgical patients [33]. It causes two types of foodborne illness: an emetic type, due to an emetic toxin, and a diarrheal type, caused by enterotoxins such as CytK, with toxin production (Hbl, Nhe, CytK) regulated by the PlcR quorum sensing system; its hydrophobic spores enhance surface adherence and survival in food. Although often underreported due to mild symptoms, increased consumption of precooked and chilled foods may raise its significance as a foodborne pathogen [34]. Expanding genomic data on *B. cereus*, including studies of its pan genome and mobilome, is improving understanding of its evolution, virulence, strain variation, and adaptation, supporting better detection and control strategies [35].

Figure1.4.1: Bacillus cereus

1.4.2 Salmonella paratyphi

Salmonella paratyphi is defined as a gram-negative, rod-shaped bacterium *(Figure1.4.2)* and one of the serotypes of Salmonella that can cause systemic infections in humans. Enteric fever in India, traditionally caused by *Salmonella typhi*, is increasingly associated with *Salmonella paratyphi*.

A study from Chandigarh (2006–2007) reported a rising proportion of *S. paratyphi* among enteric fever cases, with most isolates sensitive to ciprofloxacin and cefotaxime, though reduced ciprofloxacin susceptibility and high nalidixic acid resistance were observed; chloramphenicol sensitivity re-emerged, while ampicillin sensitivity declined. These findings establish *S. paratyphi* as an emerging pathogen and underscore the need to reassess empirical treatment strategies due to changing resistance patterns [36]. In parts of Asia, particularly southeast China, *S. paratyphi* is now more frequently isolated than S. Typhi, suggesting its growing role as a major cause of enteric fever, possibly due to either rising *S. paratyphi* infections or declining *S. typhi* cases from vaccination, though long-term surveillance data are limited [37]. Human challenge studies indicate that prior *S. paratyphi* infection reduces risk and delays disease upon re-exposure but does not provide full protection, with some individuals naturally more resistant; prior *S. typhi* infection offers no cross-protection against *S. paratyphi*, and antibody responses and symptoms were similar in primary and secondary infections, highlighting the need for improved vaccines targeting both pathogens [38].

Figure1.4.2: Salmonella paratyphi

1.4.3 *Klebsiella pneumoniae*

Klebsiella pneumoniae is a Gram-negative bacterium *(Figure1.4.3)* belonging to the family Enterobacteriaceae, is typically an opportunistic, hospital-acquired pathogen affecting immunocompromised individuals. However, hypervirulent strains with increased capsule production can infect healthy people, causing severe community-acquired diseases such as liver abscess, meningitis, endophthalmitis, necrotizing fasciitis, and pneumonia. Its pathogenicity is driven by virulence factors including capsule polysaccharide, lipopolysaccharide, fimbriae, outer membrane proteins, and iron acquisition systems, which promote survival and immune evasion [39]. *K. pneumoniae* is a major cause of pneumonia, urinary tract, and bloodstream infections, and the emergence of multidrug-resistant and carbapenem-resistant strains mainly due to β-lactamase production has made treatment difficult. Although vaccine candidates such as Kleb4V are under study, no approved vaccine exists. Rising resistance rates, particularly in China, underscore the need for better surveillance and control strategies [40]. The pathogen's global health threat is exacerbated by antimicrobial resistance mechanisms, including extended-spectrum β-lactamase production and efflux pumps, prompting exploration of novel strategies such as bacteriophage therapy, CRISPR-Cas systems, antimicrobial peptides, and targeting virulence factors or biofilm formation are being explored as alternative approaches to combat this pathogen [41].

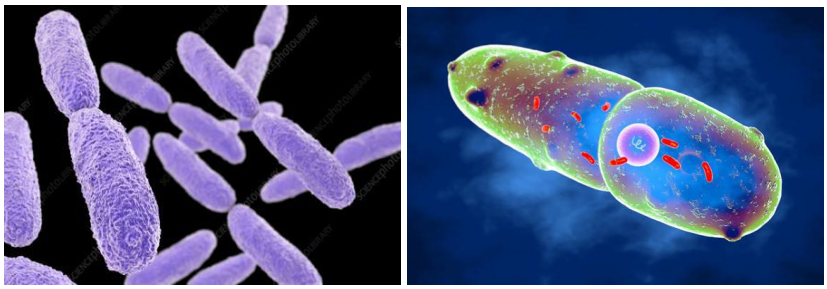

Figure1.4.3: Klebsiella pneumoniae

1.4.4 *Vibrio parahaemolyticus*

Vibrio parahaemolyticus is a Gram-negative marine bacterium *(Figure1.4.4)* and a major food-borne pathogen acquired through raw or undercooked seafood. Its virulence factors—including hemolysin, urease, and type III and type VI secretion systems—cause cytotoxic and enterotoxic effects. Detection methods targeting these factors aid in monitoring seafood safety. Understanding its pathogenic mechanisms supports improved diagnosis, prevention, and treatment of infections in humans [42]. It is a marine bacterium commonly found in raw seafood, especially shellfish. Eating contaminated raw or undercooked seafood can cause acute gastroenteritis with diarrhea, nausea, vomiting, headache, and abdominal cramps. It is a major cause of seafood-related foodborne illness in many Asian countries and the leading cause in the United States [43].

It causes diseases in marine aquaculture, resulting in significant economic losses, and is a leading cause of seafood-borne diarrheal illness in humans worldwide. Advances in animal models, next-generation sequencing, and biochemical and cell biology techniques have improved understanding of its pathogenic mechanisms. Its virulence is linked to multiple factors, including hemolysin, type III and type VI secretion systems, adhesion factors, iron uptake systems, lipopolysaccharides, proteases, and outer

membrane proteins. These virulence factors represent potential targets for new therapeutic and preventive strategies [44].

Figure1.4.4: Vibrio parahaemolyticus

1.4.5 *Escherichia coli (E. coli)*

Escherichia coli is a Gram-negative, rod-shaped (bacillus) bacterium *(Figure1.4.5)* belonging to the family Enterobacteriaceae. It is a common commensal inhabitant of the gastrointestinal tract of humans and warm-blooded animals but also a major pathogen responsible for enteritis, urinary tract infections, septicaemia, neonatal meningitis, and diarrhoea in pets and farm animals. The increasing emergence of multidrug-resistant strains, mainly due to mobile genetic elements such as plasmids, poses a significant public health concern worldwide, particularly in Europe. Despite its pathogenic potential, *E. coli* is widely used in biotechnology because of its well-characterized genome, ease of cultivation under both aerobic and anaerobic conditions, and extensive application in industrial, medical, and recombinant DNA technology [45].

It causes diarrheagenic infections cause watery diarrhea and abdominal cramps through intestinal colonization, toxin production, and tissue damage. Some strains produce Shiga toxins similar to those of Shigella dysenteriae. Contamination usually originates from animal feces and spreads to food, water, and processing environments. Improved food

control measures, rapid detection methods, and enhanced surveillance have strengthened outbreak identification and prevention [46]. Its virulence factors disrupt host processes such as cell signalling, ion secretion, protein synthesis, mitosis, and cytoskeletal and mitochondrial functions. These genes are often located on mobile genetic elements like plasmids, bacteriophages, transposons, and pathogenicity islands, enabling the emergence of new virulent strains. Pathogenic strains show a mosaic genome structure and regulate virulence through both pathotype-specific and housekeeping regulators [47].

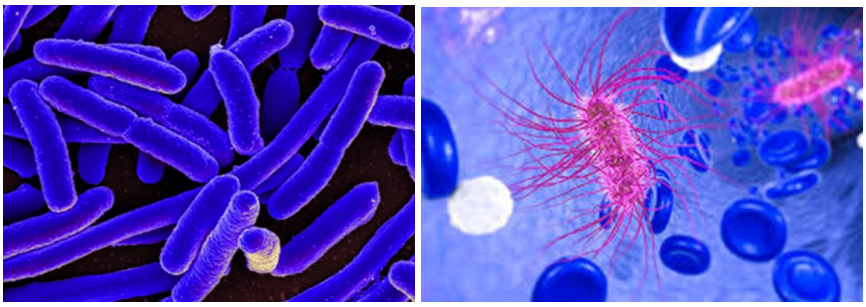

Figure1.4.5: Escherichia coli (E. coli)

1.4.6 *Staphylococcus aureus*

Staphylococcus aureus is a Gram-positive, spherical bacterium *(Figure1.4.6)* that causes a wide range of severe diseases. It normally inhabits the skin and nasopharynx of humans but can cause a wide range of infections affecting skin, soft tissues, bloodstream, and internal organs, leading to significant morbidity and mortality in both community and hospital settings. It can spread from superficial sites through the bloodstream to form metastatic infections, particularly in surgical wounds and on indwelling medical devices. It also causes food poisoning through enterotoxin-contaminated food and is responsible for economically

important ruminant mastitis. Its pathogenicity is linked to numerous virulence factors that contribute to infection and disease progression [48].

Staphylococcal food poisoning is mainly caused by toxins produced by *Staphylococcus aureus* and is an intoxication rather than an infection. Humans are the primary reservoir, and the bacterium can develop resistance to antibiotics. Its enterotoxins act as superantigens, binding to MHC II and T-cell receptors, and are resistant to gastric enzymes, allowing them to survive in the gut and cause illness. Advances in molecular studies have improved understanding of the mechanisms underlying this foodborne disease [49]. Its virulence is largely due to numerous secreted toxins that damage cell membranes and induce cell death, including hemolysins and leukotoxins. Some leukotoxins can lyse neutrophils even after phagocytosis, enabling the bacterium to evade innate immune defenses. It also produces factors that inhibit the complement system and prevent immune recognition. Recent research has clarified how its leukotoxins function through both receptor-mediated and receptor-independent mechanisms to enhance pathogenicity [50].

Figure1.4.6: Staphylococcus aureus

Chapter 2

Materials and Methods

This chapter gives a brief description of the materials and experimental procedures adopted for the present investigation.

2.1 MATERIALS

2.1.1 Reagents

1. Quercetin
2. 2-amino-5methylpyridine
3. 2-amino-4nitrophenol
4. 3-aminobenzoic acid
5. Sulphanilamide

2.1.2 Solvents

1.Methanol
2.Ethanol
3.Petroleum ether
4. DMSO

2.2 EXPERIMENTAL METHODS

2.2.1 Elemental Analysis

Elemental Analysis (CHN) is a fundamental analytical technique used to determine the mass percentages of carbon, hydrogen, and nitrogen within

an organic sample, serving as a primary tool for establishing chemical identity and purity. The general process involves the rapid combustion of a micro-sample at temperatures exceeding 900°C in an oxygen-rich environment, which converts the organic elements into simple gases: carbon dioxide, water vapor, and nitrogen gas. These gases are then separated and quantified using a thermal conductivity detector, allowing the instrument to calculate the exact weight percentage of each element present. In conclusion, this analysis provides the essential empirical data needed to verify a compound's molecular formula and ensure that the synthesized materials meet specific quality standards, making it an indispensable resource in chemical research and industrial manufacturing.

Carbon, hydrogen and nitrogen content in all the synthesized compounds were analysed by using a Vario EL CHNS analyser at Sophisticated Test Instrumentation Centre (SAIF), CUSAT.

2.2.2 UV-Visible Spectroscopy

UV–Visible Spectroscopy is an analytical technique used to determine the chemical properties and concentration of substances by measuring light absorption in the ultraviolet (190–400 nm) and visible (400–800 nm) regions. It is based on electronic transitions, where electrons absorb energy and move from ground states (bonding or non-bonding orbitals) to excited states (anti-bonding orbitals).

Characteristic absorption peaks arise from electronic transitions such as $\pi \rightarrow \pi^*$ in unsaturated compounds and $n \rightarrow \pi^*$ transitions in certain functional groups. These peaks act as fingerprints for identifying chromophores. In practice, a light beam passes through the sample, and the detector measures absorbance to generate a spectrum used for qualitative and quantitative analysis.

It studies how molecules absorb energy, promoting electrons to higher energy levels. The spectrum is obtained by plotting wavelength against absorbance or molar absorptivity (ε). Electronic transitions are often accompanied by vibrational and rotational changes, contributing to the overall spectral pattern.

The UV–Visible region spans approximately 200–800 nm and includes the far UV (10–200 nm), near UV (200–380 nm), and visible region (380–780 nm). The far UV requires vacuum conditions, while the near UV can be studied using quartz optics. Increased conjugation shifts absorption to longer wavelengths, sometimes into the visible region, producing coloured compounds such as β-carotene (≈451 nm).

The UV–Visible spectra of the synthesized samples were recorded in methanol using a Thermo Electron Nicolet Evolution 300 UV–Vis spectrophotometer [51].

2.2.3 FT-IR Spectroscopy

Fourier Transform Infrared (FT-IR) Spectroscopy is a high-precision analytical technique used to identify organic, polymeric, and in some cases, inorganic materials by measuring how they absorb infrared radiation. The method is based on the excitation of vibrational transitions within a molecule; when the frequency of the incoming infrared light matches the natural vibrational frequency of a chemical bond, the energy is absorbed, causing the bond to stretch or bend.

These transitions are specific to the types of atoms and the strength of the bonds involved, such as the distinct stretching of a carbonyl group or the bending of a hydroxyl group, effectively creating a unique "molecular fingerprint" for the substance. Unlike traditional scanning methods, FT-IR

utilizes an interferometer to collect all spectral data simultaneously, which a computer then decodes into a readable spectrum of absorption peaks.

Spectrometer in the range 4000-400 cm^{-1} using KBr pellets at the central Instrumentation Facility in Bharat Mata College.

2.2.4 Nuclear Magnetic Resonance Spectroscopy

Nuclear Magnetic Resonance (NMR) Spectroscopy is an advanced analytical technique used to determine molecular structure by studying the magnetic properties of atomic nuclei, mainly ^{1}H and ^{13}C. When a sample is placed in a strong magnetic field and exposed to radiofrequency radiation, nuclei with spin absorb energy and transition to higher energy states. The required energy depends on the surrounding electron density (shielding), producing chemical shifts measured in ppm.

Chemical shifts reveal functional groups and molecular environments. In ^{1}H NMR, signals at 0.5–2.0 ppm usually correspond to aliphatic protons, 6.0–8.5 ppm to aromatic protons, and above 9.0 ppm to aldehydes or acids. In ^{13}C NMR, carbonyl carbons typically appear between 160–220 ppm. Thus, NMR provides detailed information about atom connectivity and molecular symmetry.

NMR spectroscopy examines differences in magnetic environments within molecules, enabling determination of structural, mechanistic, and stereochemical details. In ^{1}H NMR, it reveals the number of distinct hydrogen environments, neighbouring proton interactions (splitting patterns), and relative proton ratios through signal integration.

The resonance frequency varies with chemical environment, resulting in distinct signals for different nuclei. For example, toluene shows separate signals for methyl and aromatic protons. Similarly, ^{13}C NMR identifies

different carbon environments. Together, ^{1}H and ^{13}C NMR spectroscopy provide comprehensive structural information for organic compounds[52]. The ^{1}H and ^{13}C NMR spectra detected using $CDCl_3$ on a Bruker Advance DRX 300NFT-NMR Spectrometer at SAIF, CUSAT with TMS as the standard.

2.2.5 Antibacterial Study

The antibacterial study was carried out using a systematic approach to assess the efficacy of the tested compounds. Nutrient media was prepared by dissolving 1.3 g of nutrient broth in 100 ml of distilled water, with 5 ml dispensed into test tubes and sterilized using an autoclave. Nutrient agar was prepared by mixing 1.3 g of nutrient broth and 2 g of agar in 100 ml of distilled water, autoclaved, and 20 ml poured into sterile Petri plates under aseptic conditions. The test organisms were inoculated into 5 ml of sterilized nutrient broth and incubated overnight at 37°C. For the well diffusion assay, a lawn culture of each bacterium was prepared by spreading bacterial suspension over the agar surface using sterile cotton swabs in both directions to cover the entire plate. Wells of 6 mm diameter were cut into the agar, labeled, and loaded with 20 µL of each sample. The antibacterial activity was compared with standard antibiotics, and plates were incubated at 37°C for 24 hours. The radius of the inhibition zones was measured in centimeters; a clear zone around the well indicates bacterial growth inhibition, with larger zones reflecting higher compound effectiveness. After the experiment, all bacteria were destroyed by autoclaving the plates for 20 minutes, and all glassware was sterilized to ensure complete removal of any remaining bacteria.

2.3 SYNTHESIS OF SCHIFF BAS ES

2.3.1 Synthesis of Schiff base from Quercetin and 3-aminobenzoic acid (QABD)

Quercetin and 3-aminobenzoic acid in methanol were combined in 1:1 ratio and heated for 6 hours under reflux in a round-bottom flask (Scheme1). After cooling and being concentrated, the obtained solution is allowed to undergo slow evaporation. The precipitate collected after filtering, and washing with ethanol is recrystallized and dried. Crystals with a yellow hue were obtained (*Figure2.1*)**.**

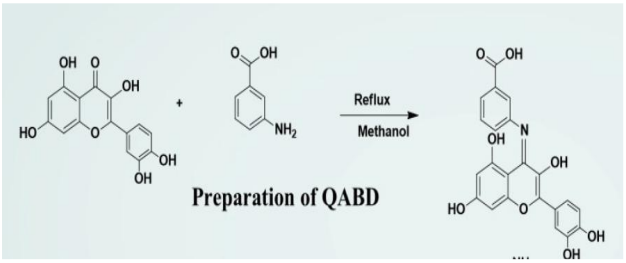

Scheme 1: Preparation of Schiff base QABD

Figure2.1: Crystals of QABD

2.3.2 Synthesis of Schiff base from Quercetin and 2-amino-5methylpyridine (QAMP)

Quercetin and 2-amino-5methylpyridine in methanol were combined in 1:1 ratio and heated for 6 hours under reflux in a round-bottom flask (Scheme 2). After cooling and being concentrated, the obtained solution is allowed to undergo slow evaporation. The precipitate collected after filtering, and washing with ethanol is recrystallized and dried. Crystals with a yellow hue were obtained (*Figure2.2*).

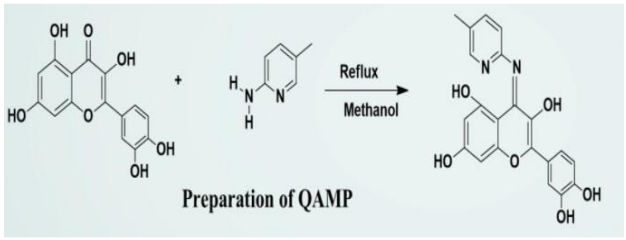

Scheme 2: Preparation of Schiff base QAMP

Figure2.2: Crystals of QAMP

2.3.3 Synthesis of Schiff base from Quercetin and Sulfanilamide (QSAM)

Quercetin and Sulfanilamide in methanol were combined in 1:1 ratio and heated for 6 hours under reflux in a round-bottom flask (Scheme 3). After cooling and being concentrated, the obtained solution is allowed to undergo slow evaporation. The precipitate collected after filtering, and washing with ethanol is recrystallized and dried. Crystals with a yellow hue were obtained (*Figure2.3*).

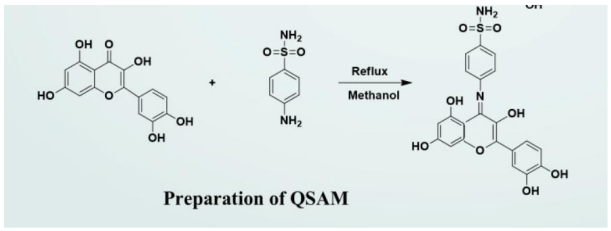

Scheme 3: Preparation of Schiff base QSAM

Figure2.3: Crystals of QSAM

2.3.4 Synthesis of Schiff base from Quercetin and amino nitrophenol (QANP)

Quercetin and amino nitrophenol in methanol were combined in 1:1 ratio and heated for 6 hours under reflux in a round-bottom flask (Scheme 4). After cooling and being concentrated, the obtained solution is allowed to undergo slow evaporation. The precipitate collected after filtering, and washing with ethanol is recrystallized and dried. Crystals with a yellow hue were obtained (*Figure2.4*).

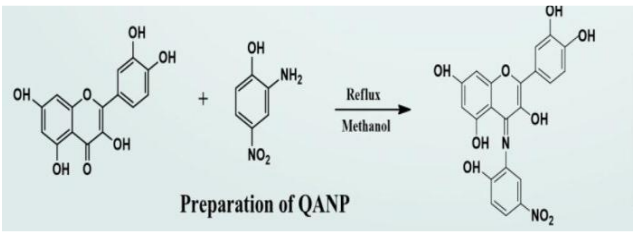

Scheme 4: Preparation of Schiff base QANP

Figure2.4: Crystals of QANP

Chapter 3

Results and Discussion

3.1 ANALYSIS OF QABD (Quercetin+3-aminobenzoic acid)

3.1.1 Elemental Analysis

Elemental analysis of QABD was conducted to examine the elemental composition of the Schiff base. QABD has an empirical formula $C_{22}H_{15}O_8N$. The results obtained are consistent with the proposed chemical formula of the assigned structure (*Table 1*).

Compound	Empirical Formula	Formula Weight	Colour	Calculated (Observed %)		
				C	H	N
QABD	$C_{22}H_{15}O_8N$	421.366	Yellow	63.45 (65.72)	3.94 (4.11)	3.22 (3.46)

Table 1: Elemental analysis of QABD

3.1.2 UV-Visible Spectroscopy

The chemical structure and optical characteristics of the sample QABD were investigated using Ultraviolet-visible spectroscopy. The UV-visible spectrum of QABD was obtained in methanol (*Figure3.1*). In the UV-visible spectrum, the primary transitions are $\pi \rightarrow \pi^*$ for aromatic rings around 180–350 nm and $n \rightarrow \pi^*$ for azomethine groups (C=N) around 300–450 nm. The sample QABD exhibit peaks at 260 nm for transition within aromatic rings and 370 nm for transition within C=N group.

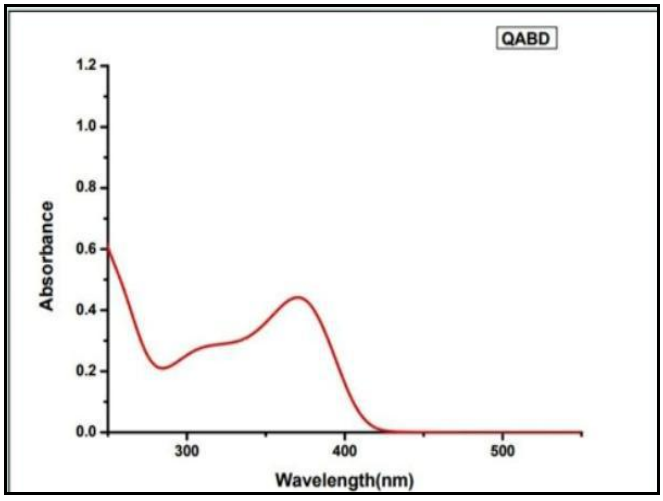

Figure3.1: UV-visible spectrum of QABD

3.1.3 Infrared Spectroscopy

The functional groups present and molecular structure of the sample QABD were obtained from IR spectrum (*Figure3.2*). A sharp peak at 1653.90 cm^{-1} was obtained for QABD corresponding to the IR absorption peak of imine group (C=N) in the range 1690–1640 cm^{-1}. A peak at 3405.71 cm^{-1} was obtained corresponding to the absorption peak of phenolic (OH) group in the range 3500–3200 cm^{-1}.

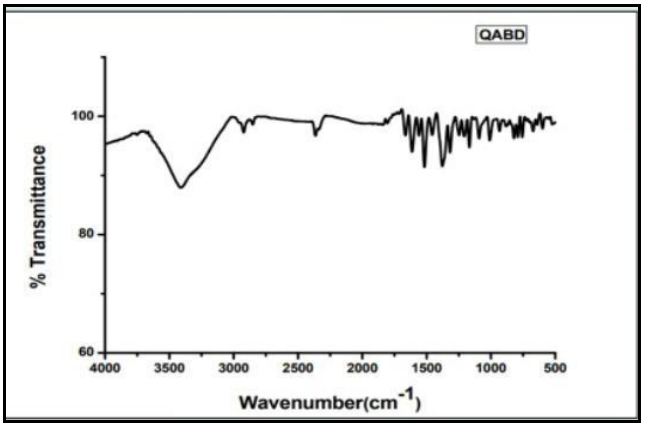

Figure3.2: IR spectrum of QABD

3.1.4 Nuclear Magnetic Resonance Spectroscopy

3.1.4.1 ^{1}H NMR Spectroscopy

^{1}H NMR spectrum of QABD provides the information about the number of hydrogen atoms and their relationships (*Figure3.3*).

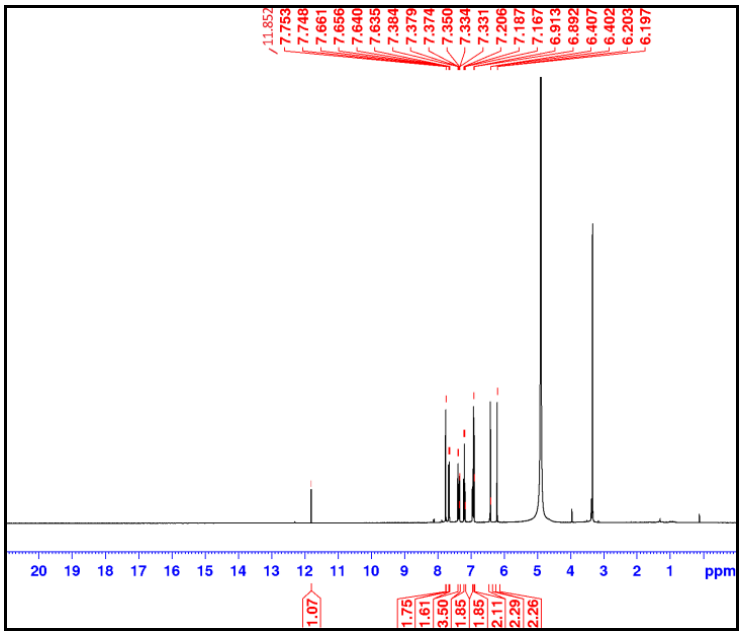

Figure3.3: ^{1}H NMR spectrum of QABD

^{1}H NMR (CH_3OH δ ppm): 6.2(2H, Ar-H), 6.9(2H, Ar-H), 6.8(2H, Ar-H), 6.9(1H, Ar-H), 7.1(1H, Ar-H), 7.2(2H, OH), 7.3(1H, OH), 7.6(2H, OH), 7.7(1H, OH), 11.8(1H, CH_3COOH).

3.1.4.2 ^{13}C NMR Spectroscopy

^{13}C NMR spectrum of the sample QABD reveal the carbon skeleton of the compound (*Figure3.4*)**.**

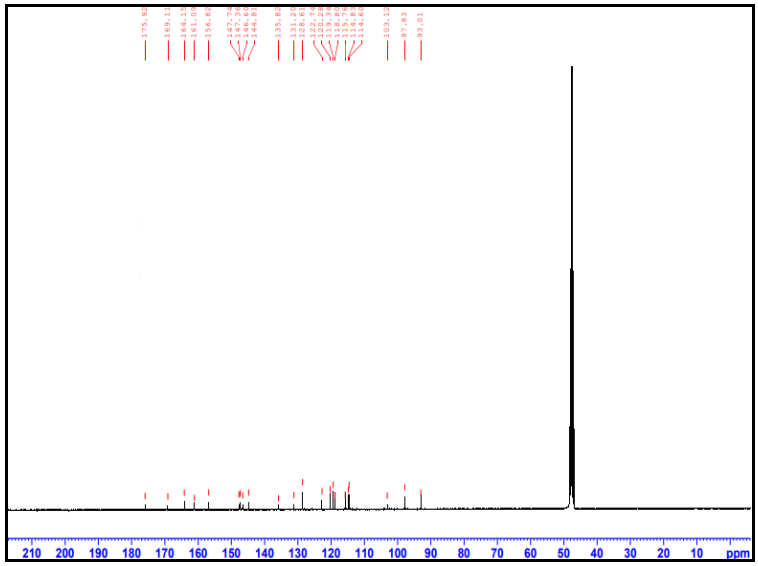

Figure3.4: ^{13}C NMR spectrum of QABD

^{13}C NMR (CH_3OH δ ppm): 93.70 (Ar-C), 98.63 (Ar-C), 104.23 (Ar-C), 114.29, 116.79 (Ar-C), 120.031 (Ar-C), 122.49 (Ar-C), 130.28 (Ar-C), 132.46 (Ar-H), 136.24 (Ar-H), 147.22 (Ar-C-OH), 148.23 (Ar-C-OH), 157.65 (Ar-CO), 161.27 (Ar-C-OH), 168.15 (Ar-C-OH), 169.11 (Ar-C-OH), 175.92 (Ar-C=N).

3.2 ANALYSIS OF QSAM (Quercetin+Sulfanilamide)

3.2.1 Elemental Analysis

Elemental analysis of QSAM was conducted to examine the elemental composition of the Schiff base. QSAM has an empirical formula $C_{21}H_{16}O_8N_2S$. The results obtained are consistent with the proposed chemical formula of the assigned structure (*Table 2*).

Compound	Empirical Formula	Formula Weight	Colour	Calculated (Observed %)		
				C	H	N
QSAM	$C_{21}H_{16}O_8N_2S$	456.434	Greenish Yellow	56.06 (55.89)	4.36 (4.87)	5.31 (5.90)

Table 2: Elemental analysis of QSAM

3.2.2 UV-Visible Spectroscopy

The chemical structure and optical characteristics of the sample QSAM were investigated using Ultraviolet-visible spectroscopy. The UV-visible spectrum of QSAM was obtained in methanol (*Figure3.5*). In the UV-visible spectrum, the primary transitions are π→π* for aromatic rings around 180–350 nm and n→π* for azomethine groups (C=N) around 300–450 nm. The sample QSAM exhibit peaks at 268 nm for transition within aromatic rings and 369 nm for transition within C=N group.

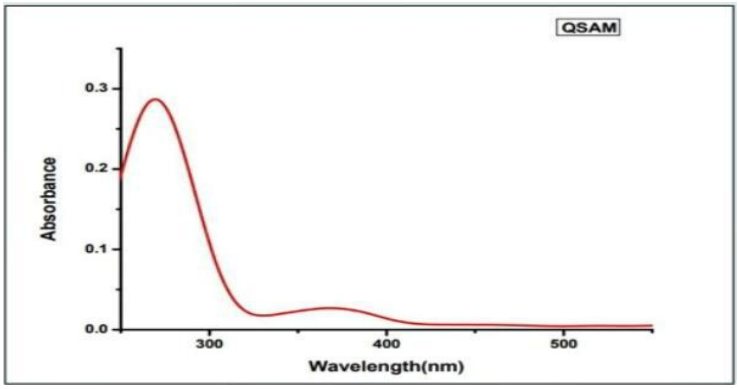

Figure3.5: UV-visible spectrum of QSAM

3.2.3 Infrared Spectroscopy

The functional groups present and molecular structure of the sample QSAM were obtained from IR spectrum (*Figure3.6)*. A sharp peak at 1653.85 cm^{-1} was obtained for QSAM corresponding to the IR absorption peak of imine group (C=N) in the range 1690–1640 cm^{-1}. A peak at 3420.19 cm^{-1} was obtained corresponding to the absorption peak of phenolic (OH) group in the range 3500–3200 cm^{-1}.

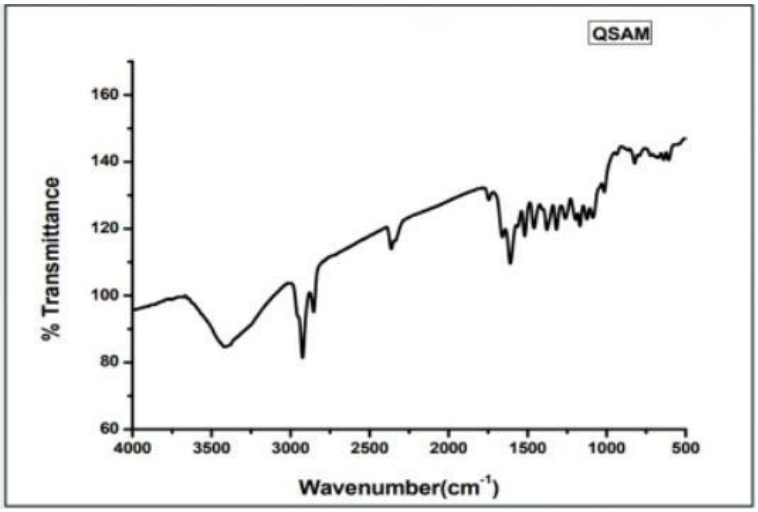

Figure3.6: IR spectrum of QSAM

3.2.4 Nuclear Magnetic Resonance Spectroscopy

3.2.4.1 ^{1}H NMR Spectroscopy

^{1}H NMR spectrum of QSAM provides the information about the number of hydrogen atoms and their relationships (*Figure3.7*).

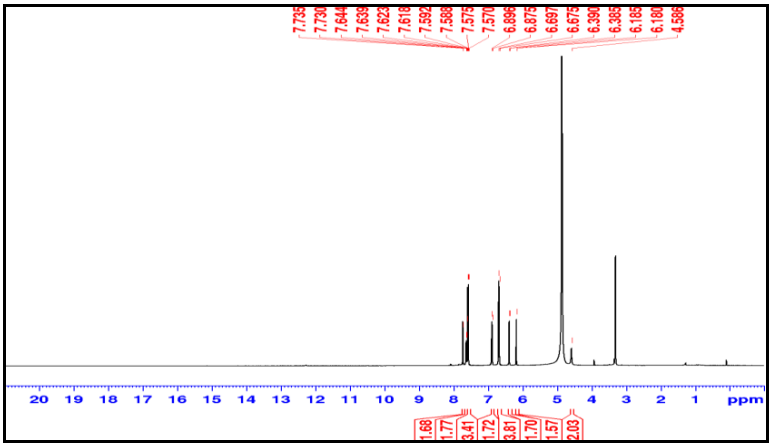

Figure3.7: [1]H NMR spectrum of QSAM

[1]H NMR (CH_3OH δ ppm): 4.58 (2H, N-H), 6.1 (2H, Ar-H), 6.3 (1H, Ar-H), 6.6 (2H, Ar-H), 6.8 (2H, Ar-H), 7.5 (2H, Ar-H), 7.6 (2H, Ar-OH), 7.7 (2H, OH), 7.8 (1H, OH).

3.2.4.2 [13]C NMR Spectroscopy

[13]C NMR spectrum of the sample QSAM reveal the carbon skeleton of the compound (*Figure3.8*).

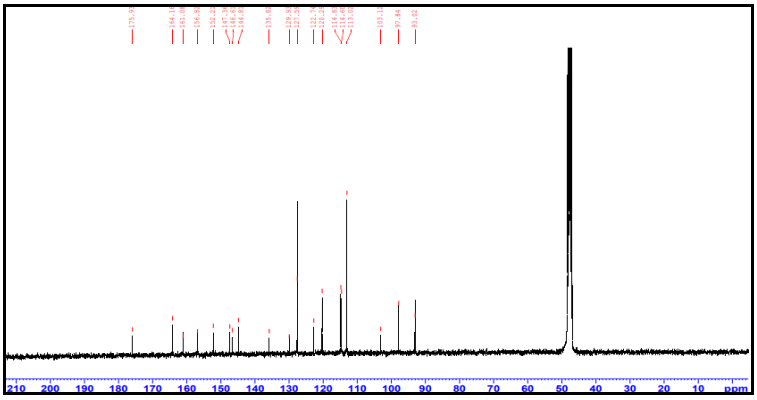

Figure3.8: [13]C NMR spectrum of QSAM

^{13}C NMR (CH_3OH δ ppm): 93.02 (Ar-C), 97.84 (Ar-C), 103.12 (Ar-C), 113.02, 114.60 (Ar-C), 120.29 (Ar-C), 122.74 (Ar-C), 129.39 (Ar-OH), 135.82 (Ar-OH), 144.81 (Ar-OH), 146.61 (Ar-C-OH), 152.21 (Ar-CO), 161.08 (Ar-C-OH), 175.53 (Ar-C=N).

3.3 ANALYSIS OF QAMP (Quercetin+2-amino-5-methylpyridine)

3.3.1 Elemental Analysis

Elemental analysis of QAMP was conducted to examine the elemental composition of the Schiff base. QAMP has an empirical formula $C_{21}H_{16}O_6N_2$. The results obtained are consistent with the proposed chemical formula of the assigned structure (*Table 3*).

Compound	Empirical Formula	Formula Weight	Colour	Calculated (Observed %)		
				C	H	N
QAMP	$C_{21}H_{16}O_6N_2$	392.369	Yellow	64.45 (64.98)	3.86 (3.97)	7.16 (7.25)

Table 3: Elemental analysis of QAMP

3.3.2 UV-Visible Spectroscopy

The chemical structure and optical characteristics of the sample QAMP were investigated using Ultraviolet-visible spectroscopy. The UV-visible spectrum of QAMP was obtained in methanol (*Figure3.9*). In the UV-visible spectrum, the primary transitions are π→π* for aromatic rings around 180–350 nm and n→π* for azomethine groups (C=N) around 300–450 nm. The sample QAMP exhibit peaks at 260 nm for transition within aromatic rings and 377 nm for transition within C=N group.

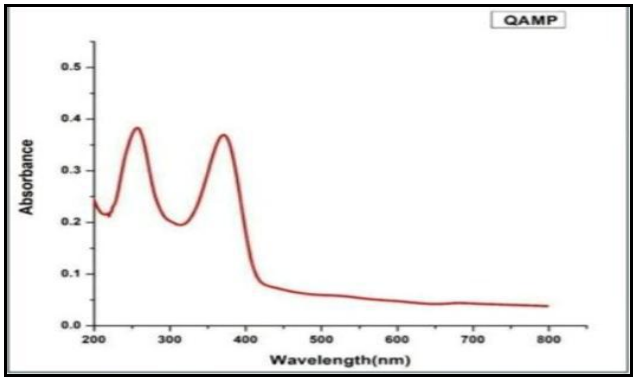

Figure3.9: UV-visible spectrum of QAMP

3.3.3 Infrared Spectroscopy

The functional groups present and molecular structure of the sample QAMP were obtained from IR spectrum (*Figure3.10*). A sharp peak at 1662.10 cm^{-1} was obtained for QAMP corresponding to the IR absorption peak of imine group (C=N) in the range 1690–1640 cm^{-1}. A peak at 3405.67 cm^{-1} was obtained corresponding to the absorption peak of phenolic (OH) group in the range 3500–3200 cm^{-1}.

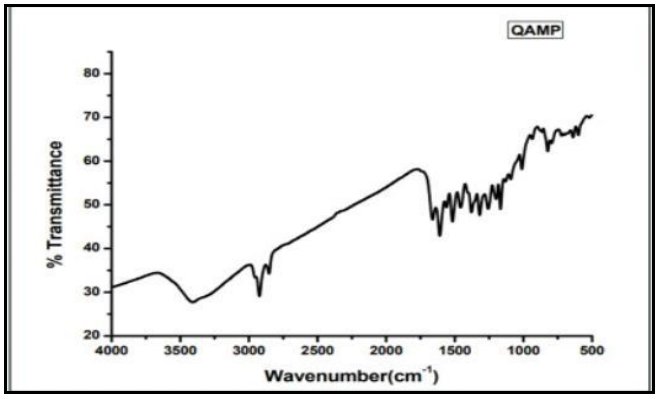

Figure3.10: IR spectrum of QAMP

3.3.4 Nuclear Magnetic Resonance Spectroscopy

3.3.4.1 ^{1}H NMR Spectroscopy

^{1}H NMR spectrum of QAMP provides the information about the number of hydrogen atoms and their relationships (*Figure3.11*).

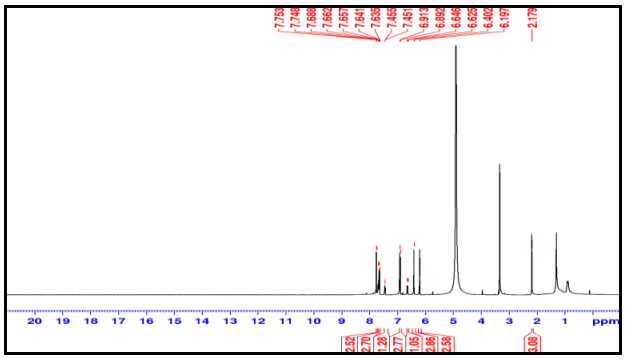

Figure3.11: ^{1}H NMR spectrum of QAMP

^{1}H NMR (CH_3OH δ ppm): 2.1 (3H, C-H), 6.2 (1H, Ar-H), 6.4 (2H, Ar-H), 6.6 (1H, Ar-H), 6.8 (2H, Ar-H), 6.9 (1H, Ar-H), 7.2 (1H, Ar-H), 7.4 (1H, OH), 7.6 (2H, OH), 7.7 (1H, OH), 7.8 (2H, OH).

3.3.4.2 ^{13}C NMR Spectroscopy

^{13}C NMR spectrum of the sample QAMP reveal the carbon skeleton of the compound (*Figure3.12*).

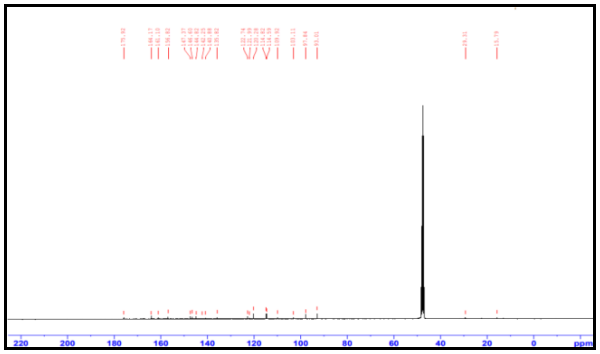

Figure3.12: ^{13}C NMR spectrum of QAMP

^{13}C NMR (CH_3OH δ ppm): 29.31 (C-H), 93.01 (Ar-C), 97.84 (Ar-C), 103.12 (Ar-C), 109.92 (Ar-C), 114.59, 114.82 (Ar-C), 120.28 (Ar-C), 121.99 (Ar-C), 122.74 (Ar-C), 135.82 (Ar-OH), 140.88 (Ar-OH), 144.81 (Ar-C), 146.60 (Ar-C-OH), 147.37 (Ar-CO), 156.82 (Ar-CO), 161.10 (Ar-C-OH), 175.92 (ArC=N).

3.4 ANALYSIS OF QANP (Quercetin+amino nitrophenol)

3.4.1 Elemental Analysis

Elemental analysis of QANP was conducted to examine the elemental composition of the Schiff base. QANP has an empirical formula $C_{21}H_{14}N_2O_9$. The results obtained are consistent with the proposed chemical formula of the assigned structure (*Table 4*).

Compound	Empirical Formula	Formula Weight	Colour	Calculated (Observed %)		
				C	H	N
QANP	$C_{21}H_{14}N_2O_9$	438	Greenish yellow	57.54 (57.48)	3.22 (3.19)	6.39 (6.38)

Table 4: Elemental analysis of QANP

3.4.2 UV-Visible Spectroscopy

The chemical structure and optical characteristics of the sample QANP were investigated using Ultraviolet-visible spectroscopy. The UV-visible spectrum of QANP was obtained in methanol (*Figure3.13*). In the UV-visible spectrum, the primary transitions are π–π* for aromatic rings around 180-350 nm and n–π* for azomethine groups (C = N) around 300-450 nm. The sample QANP exhibits peaks at 256 nm for transitions within aromatic rings and 372 nm for transitions within the C=N group.

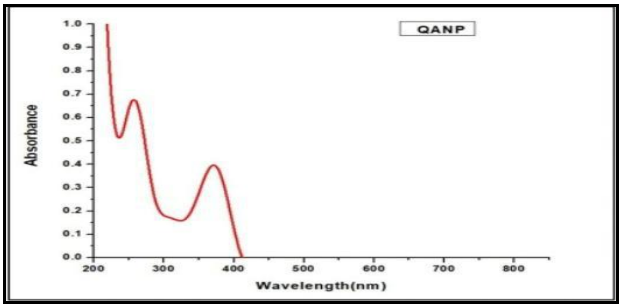

Figure3.13: UV-visible spectrum of QANP

3.4.3 Infrared Spectroscopy

The functional groups present and molecular structure of the sample QANP were obtained from IR spectrum (*Figure3.14*). A sharp peak at 1661.96 cm^{-1} was obtained for QANP corresponding to the IR absorption peak of imine group (C=N) in the range 1690-1640 cm^{-1}. A peak at 3588.05 cm^{-1} was obtained corresponding to the absorption peak of phenolic (OH) group in the range 3500-3200 cm^{-1}.

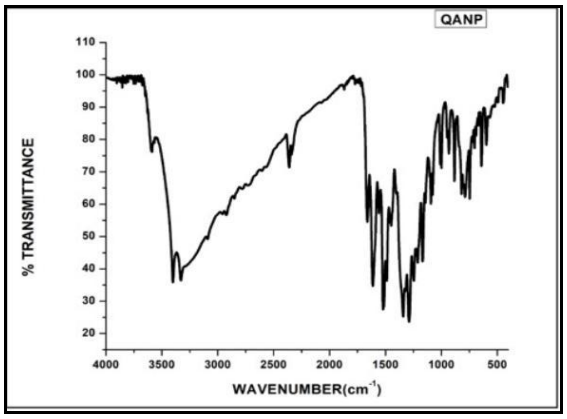

Figure3.14: IR spectrum of QANP

3.4.4 Nuclear Magnetic Resonance Spectroscopy

3.4.4.1 ^{1}H NMR Spectroscopy

^{1}H NMR spectrum of QANP provides the information about the number of hydrogen atoms and their relationships (*Figure3.15*).

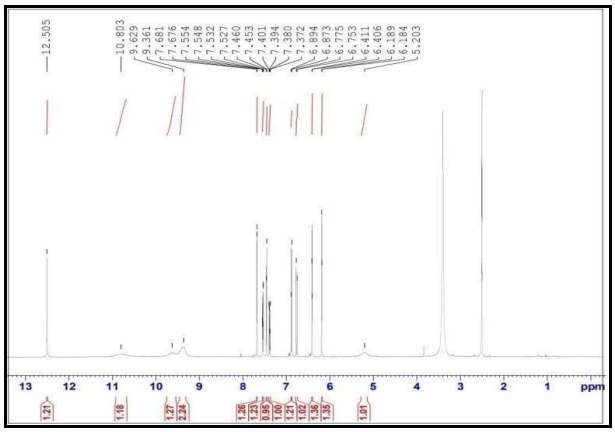

Figure3.15: ^{1}H NMR spectrum of QANP

^{1}H NMR (CH_3OH δ ppm): 12.50 (1H, OH), 10.80 (1H, CH=N), 7.75–7.30 (Ar-H), 6.18–6.90 (Ar-H), 7.40–7.80 (OH).

3.4.4.2 ^{13}C NMR Spectroscopy

^{13}C NMR spectrum of the sample QANP reveal the carbon skeleton of the compound (*Figure3.16*).

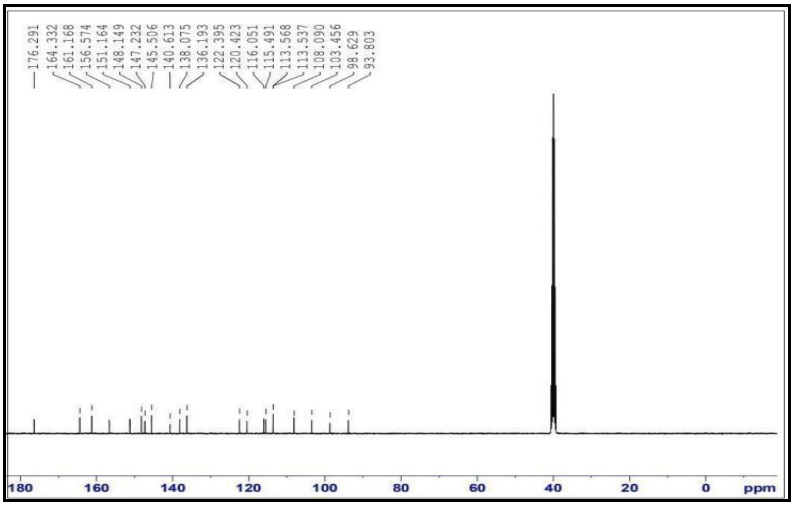

Figure3.16: ^{13}C NMR spectrum of QANP

^{13}C NMR (CH_3OH δ ppm): 176.29 (ArC=N), 164.33 (Ar-C-OH), 161.68 (Ar-C-OH), 156.12 (Ar-CO), 151.64 (Ar-C-OH), 148.12 (Ar-C-OH), 147.49 (Ar-CO), 145.50 (Ar-OH), 144.06 (Ar-C), 138.07 (Ar-C), 136.93 (Ar-C), 132.19 (Ar-C), 130.42 (Ar-C), 128.91 (Ar-C), 125.58 (Ar-C), 123.57 (Ar-C), 120.09 (Ar-C), 118.56 (Ar-C), 113.99 (Ar-C), 108.09 (Ar-C), 102.46 (Ar-C), 98.62 (Ar-C), 93.80 (Ar-C).

3.5 ANTI-BACTERIAL STUDY

The antibacterial activity of synthesized quercetin Schiff bases (QAMP, QABD, QANP, and QSAM) was evaluated using the well diffusion method. The antibacterial activity was evaluated against six bacterial strains: *Bacillus cereus, Salmonella paratyphi, Klebsiella pneumoniae, Staphylococcus aureus, Escherichia coli,* and *Vibrio parahaemolyticus* and their zone of inhibition measured (*Table 4*).

Against *Bacillus cereus*, QSAM was the most effective, producing inhibition zones of 1.1 cm, QANP at 1.0 cm, while QAMP and QABD were slightly lower at 0.8 cm. For *Salmonella paratyphi*, QAMP, QANP, and QSAM showed similar inhibition zones of 1.1 cm, with QABD slightly lower at 1.0 cm (*Figure3.17*).

In the case of *Klebsiella pneumoniae*, QABD exhibited the highest activity (1.5 cm), QSAM slightly lower at 1.4 cm, whereas QANP and QAMP were moderate (1.3 cm). Against *Staphylococcus aureus*, QANP and QSAM showed the largest inhibition zone (0.9 cm), while QAMP and QABD had lower activity (0.7 cm) (*Figure3.18*).

For *Escherichia coli*, QAMP and QABD were most potent (1.3 cm), followed by QANP (1.2 cm) and QSAM (1.1 cm). Finally, for Vibrio parahaemolyticus, QSAM demonstrated the highest activity (1.9 cm), QANP was moderate (0.9 cm), and QAMP and QABD showed minimal activity (0.7 cm) (*Figure3.19*). Six graphs were drawn to show the inhibition zones (cm) of QAMP, QABD, QANP, and QSAM against each bacterial strain, showing the inhibition zones (in cm) for each compound, which highlights their varying effectiveness across different bacteria (*Figure3.20,3.21,3.22,3.23,3.24,3.25*).

Name of Bacteria	**Zone of Inhibition in cms**				
	QAMP	QABD	QANP	QSAM	Antibiotic Disc(Gentamicin)
Bacillus cereus	0.8 cm	0.8 cm	1.0 cm	1.1 cm	2 cm
Salmonella paratyphi	1.1 cm	1.0 cm	1.1 cm	1.1 cm	2.1 cm
Klebsiella pneumoniae	1.3 cm	1.5 cm	1.3 cm	1.4 cm	1.8 cm
Staphylococcus aureus	0.7 cm	0.7 cm	0.9 cm	0.9 cm	2.7 cm
Escherichia coli	1.3 cm	1.3 cm	1.2 cm	1.1 cm	2.1 cm
Vibrio parahaemolyticus	0.7 cm	0.7 cm	0.9 cm	1.9 cm	2.8 cm

Table 4: Zone of Inhibition of synthesized compound against bacteria in cms

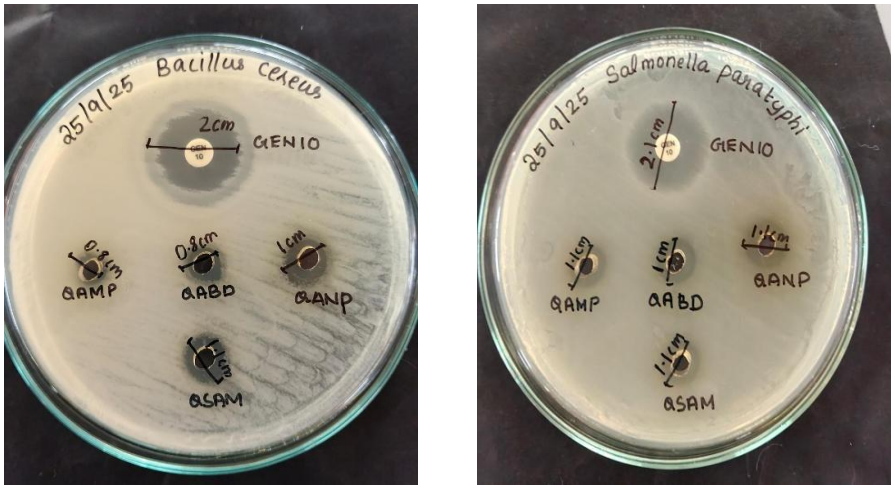

Figure3.17: Zone of Inhibition in cms of Bacillus cereus and Salmonella paratyphi

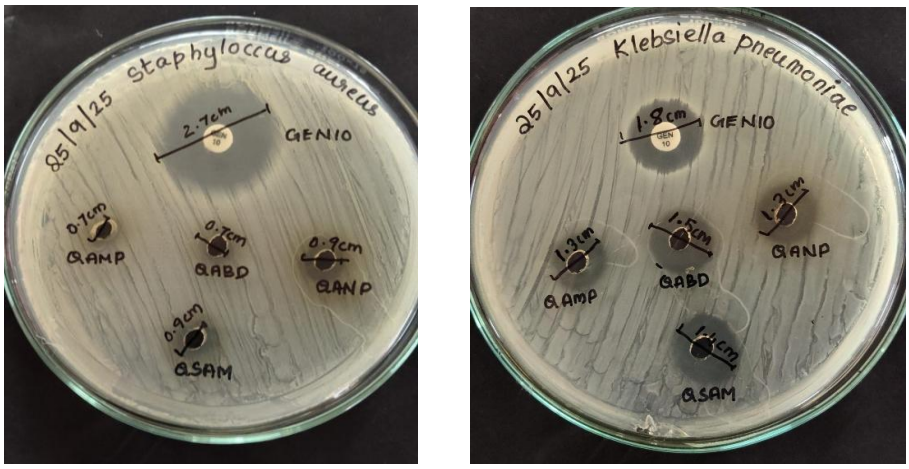

Figure3.18: Zone of Inhibition in cms of Staphylococcus aureus and Klebsiella pneumoniae

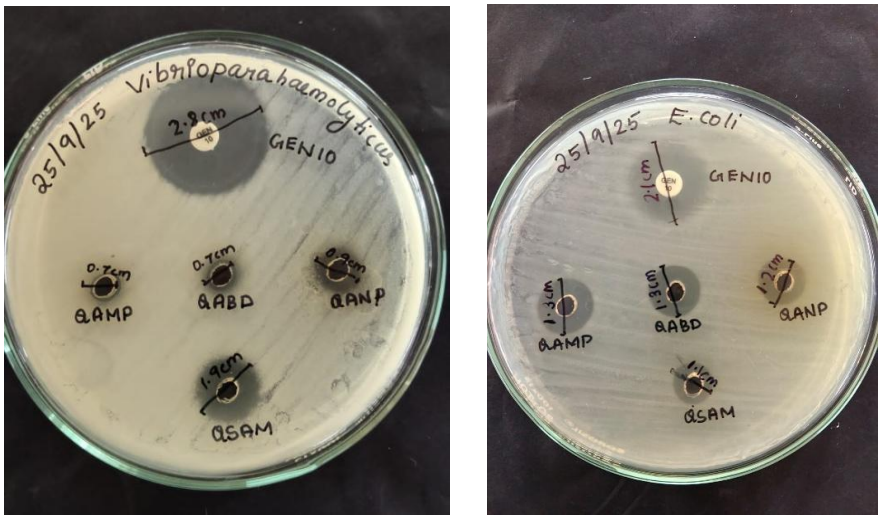

Figure3.19: Zone of Inhibition in cms of Vibrio parahaemolyticus and Escherichia coli (E. coli)

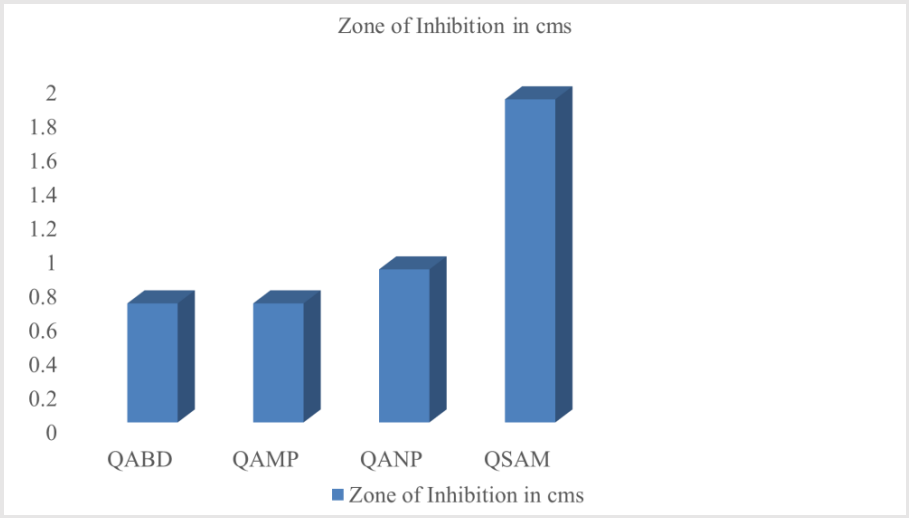

Figure3.20: Zone of Inhibition in cms of Vibrio parahaemolyticus

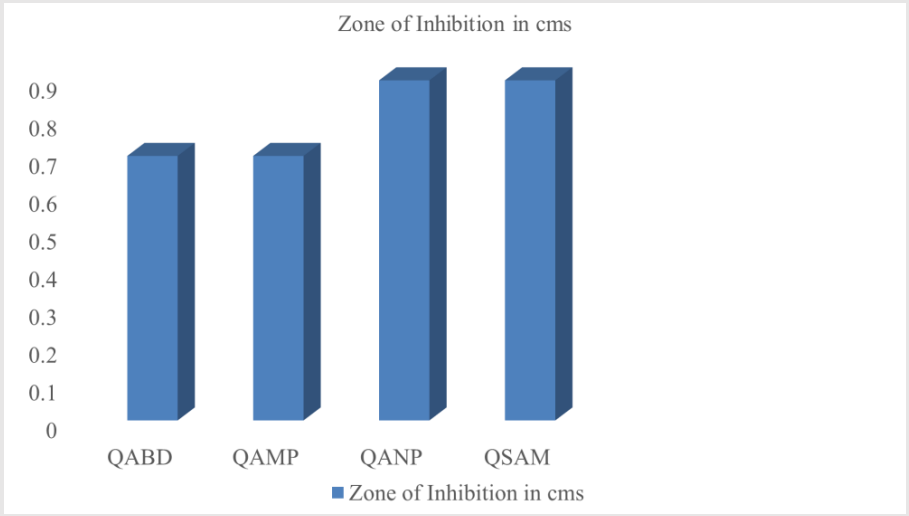

Figure3.21: Zone of Inhibition in cms of Staphylococcus aureus

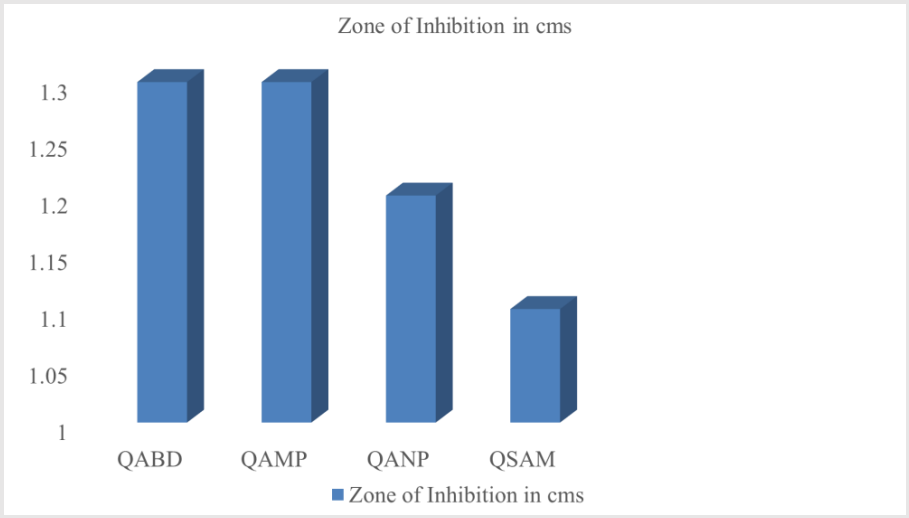

Figure3.22: Zone of Inhibition in cms Escherichia coli (E. coli)

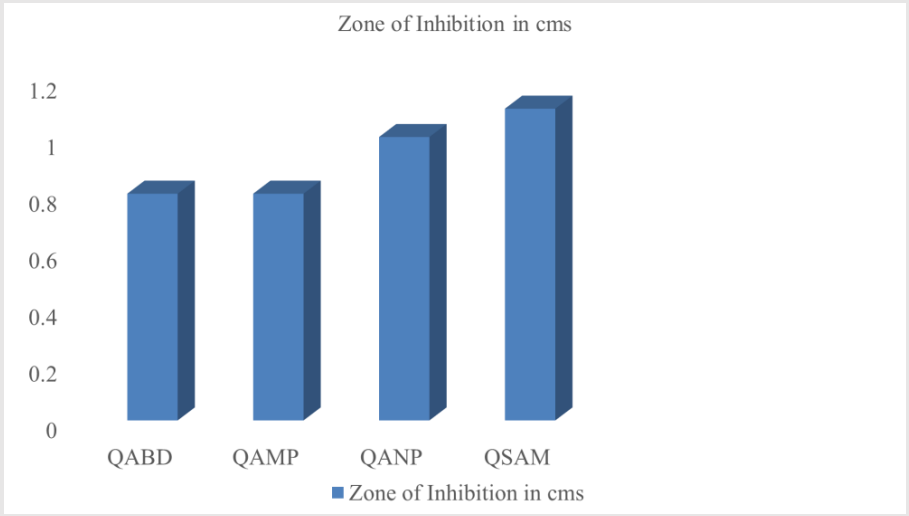

Figure3.23: Zone of Inhibition in cms of Bacillus cereus

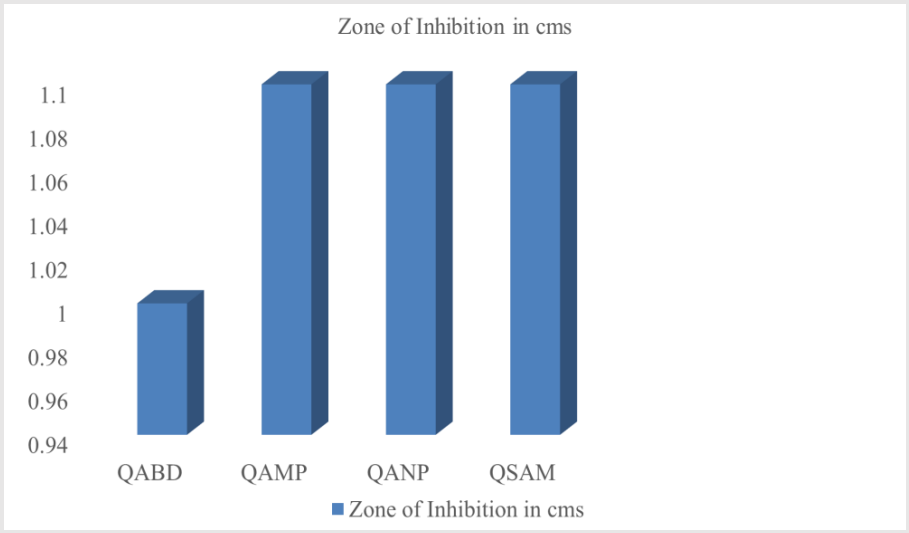

Figure3.24: Zone of Inhibition in cms of Salmonella paratyphi

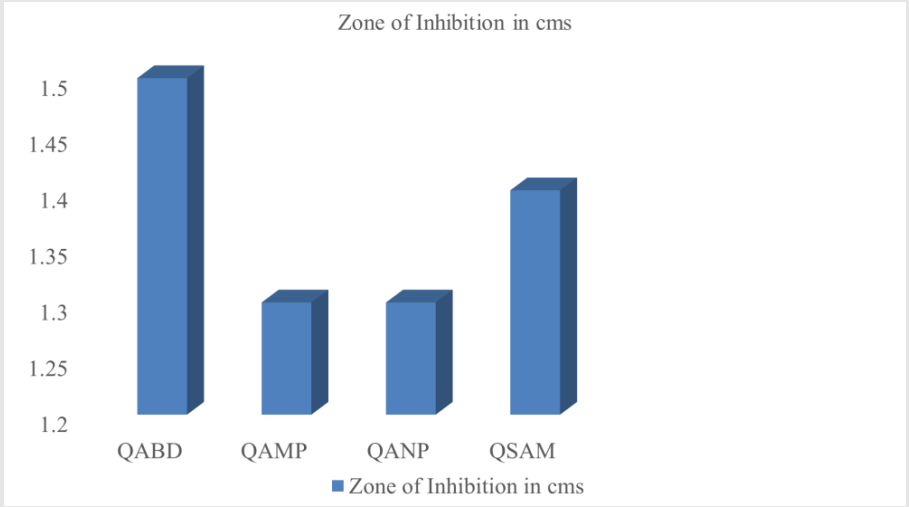

Figure3.25: Zone of Inhibition in cms of Klebsiella pneumoniae

Chapter 4

Conclusions

In this study, Quercetin-based Schiff bases (QAMP, QABD, QANP, and QSAM) were successfully synthesized, and were characterized using a range of spectroscopic techniques, including elemental analysis, UV–Visible spectroscopy, IR spectroscopy, and both ^{1}H and ^{13}C NMR spectroscopy, to confirm their structure and purity. All compounds exhibited measurable antibacterial activity against the tested strains (*Bacillus cereus, Vibrio parahaemolyticus, Klebsiella pneumoniae, Escherichia coli, Staphylococcus aureus, Salmonella paratyphi*), with effectiveness varying according to both compound structure and bacterial species. Among the derivatives, QSAM emerged as the most potent and broadly effective, particularly against *Bacillus cereus* and *Vibrio parahaemolyticus*, while QABD showed selective strength against *Klebsiella pneumoniae*, and QAMP and QABD were most effective against *Escherichia coli*. These results indicate that structural variations play a crucial role in antibacterial performance and highlight QSAM as a promising lead compound for further optimization and antimicrobial drug development. These results indicate that the antibacterial effectiveness of the compounds depends on the bacterial strain, highlighting QSAM and QANP as particularly potent against certain pathogens, while QABD exhibited selective activity against *Klebsiella pneumoniae*.

References

[1] A. Vollmannová, T. Bojňanská, J. Musilová, J. Lidiková, and M. Cifrová, "Quercetin as one of the most abundant represented biological valuable plant components with remarkable chemoprotective effects - A review," *Heliyon*, vol. 10, no. 12, 2024.

[2] M. Ay, A. Charli, H. Jin, V. Anantharam, A. Kanthasamy, and A. G. Kanthasamy, "Quercetin," *Nutraceuticals: Efficacy, Safety and Toxicity*, 2021.

[3] A. B. Bentz, "A Review of Quercetin: Chemistry, Antioxident Properties, and Bioavailability," *J. Young Investig.* 2017.

[4] P. G. Pietta, "Flavonoids as Antioxidants," *J. Nat. Prod.*, vol. 63, no. 7, 2000.

[5] X. Song, Y. Wang, and L. Gao,"Mechanism of antioxidant properties of quercetin and quercetin-DNA complex," *Journal of Molecular Modeling 2020 26:6*, vol. 26, no. 6, 2020.

[6] M. Lesjak et al., "Antioxidant and anti-inflammatory activities of quercetin and its derivatives," J. Funct. Foods, vol. 40, 2018.

[7] M. Pinelo, L. Manzocco, M. J. Nuñez, and M. C. Nicoli, "Solvent effect on quercetin antioxidant capacity," Food Chem., vol. 88, no. 2, 2004.

[8] M. Lesjak et al., "Antioxidant and anti-inflammatory activities of quercetin and its derivatives," J. Funct. Foods, vol. 40, 2018.

[9] C. F. Lin, Y. L. Leu, S. A. Al-Suwayeh, M. C. Ku, T. L. Hwang, and J. Y. Fang, "Anti-inflammatory activity and percutaneous absorption of quercetin and its polymethoxylated compound and glycosides:

The relationships to chemical structures," European Journal of Pharmaceutical Sciences, vol. 47, no. 5, 2012.

[10] V. Karuppagounder, S. Arumugam, R. A. Thandavarayan, R. Sreedhar, V. V. Giridharan, and K. Watanabe, "Molecular targets of quercetin with anti-inflammatory properties in atopic dermatitis," Drug Discov. Today, vol. 21, no. 4, 2016.

[11] R. Kleemann et al., "Anti-inflammatory, anti-proliferative and anti-atherosclerotic effects of quercetin in human in vitro and in vivo models," Atherosclerosis, vol. 218, no. 1, 2011.

[12] E. Middleton, C. Kandaswami, and T. C. Theoharides, "The Effects of Plant Flavonoids on Mammalian Cells:Implications for Inflammation, Heart Disease, and Cancer," Pharmacol. Rev., vol. 52, no. 4, 2000.

[13] M. Cruz-Correa et al., "Combination Treatment With Curcumin and Quercetin of Adenomas in Familial Adenomatous Polyposis," Clinical Gastroenterology and Hepatology, vol. 4, no. 8, 2006.

[14] A. Cossarizza et al., "Quercetin and Cancer Chemoprevention," Evidence-Based Complementary and Alternative Medicine, vol. 2011, no. 1, 2011.

[15] M. Ezzati, B. Yousefi, K. Velaei, and A. Safa, "A review on anti-cancer properties of Quercetin in breast cancer," Life Sci., vol. 248, 2020.

[16] M. Reyes-Farias and C. Carrasco-Pozo, "The Anti-Cancer Effect of Quercetin: Molecular Implications in Cancer Metabolism," International Journal of Molecular Sciences 2019, Vol. 20, Page 3177, vol. 20, no. 13, 2019.

[17] A. Rauf et al., “Anticancer potential of quercetin: A comprehensive review,” Phytotherapy Research, vol. 32, no. 11, 2018.

[18] K. M. Denny Joseph and Muralidhara, “Enhanced neuroprotective effect of fish oil in combination with quercetin against 3-nitropropionic acid induced oxidative stress in rat brain,” Prog. Neuropsychopharmacol. Biol. Psychiatry, vol. 40, no. 1, 2013.

[19] M. S. Islam et al., “Neuropharmacological Effects of Quercetin: A Literature-Based Review,” Front. Pharmacol., vol. 12, 2021.

[20] E. Akyuz, Y. N. Paudel, A. K. Polat, H. E. Dundar, and E. Angelopoulou, “Enlightening the neuroprotective effect of quercetin in epilepsy: From mechanism to therapeutic opportunities,” Epilepsy and Behavior, vol. 115, 2021.

[21] R. Kumar, S. Vijayalakshmi, and S. Nadanasabapathi, “Health benefits of quercetin,” Def. Life Sci. J, vol. 2, no. 10, 2017.

[22] P. K. Agrawal, C. Agrawal, and G. Blunden, “Quercetin: Antiviral Significance and Possible COVID-19 Integrative Considerations,” Nat. Prod. Commun., vol. 15, no. 12, 2020.

[23] T. L. A. Nguyen and D. Bhattacharya, “Antimicrobial Activity of Quercetin: An Approach to Its Mechanistic Principle,” Molecules 2022, Vol. 27, vol. 27, no. 8, 2022.

[24] S. Wang et al., “Bacteriostatic Effect of Quercetin as an Antibiotic Alternative In Vivo and Its Antibacterial Mechanism In Vitro,” J. Food Prot., vol. 81, no. 1, 2018.

[25] S. N. Pandeya, D. Sriram, G. Nath, and E. De Clercq, "Synthesis and antimicrobial activity of Schiff and Mannich bases of isatin and its derivatives with pyrimidine," Il Farmaco, vol. 54, no. 9, 1999.

[26] S. G. Giteru, R. Coorey, D. Bertolatti, E. Watkin, S. Johnson, and Z. Fang, "Physicochemical and antimicrobial properties of citral and quercetin incorporated kafirin-based bioactive films," Food Chem., vol. 168, 2015.

[27] E. Raczuk, B. Dmochowska, J. Samaszko-Fiertek, and J. Madaj, "Different Schiff Bases—Structure, Importance and Classification," Molecules 2022, Vol. 27, vol. 27, no. 3, 2022.

[28] C. M. Da Silva et al., "Schiff bases: A short review of their antimicrobial activities," J. Adv. Res., vol. 2, no. 1, 2011.

[29] A. Kajal, S. Bala, S. Kamboj, N. Sharma, and V. Saini, "Schiff Bases: A Versatile Pharmacophore," Journal of Catalysts, vol. 2013, no. 1, 2013.

[30] S. A. Dalia et al., "A short review on chemistry of schiff base metal complexes and their catalytic application," Int. J. Chem. Stud, vol. 6, no. 3, 2018.

[31] A. M. Abu-Dief and I. M. A. Mohamed, "A review on versatile applications of transition metal complexes incorporating Schiff bases," Beni. Suef. Univ. J. Basic Appl. Sci., vol. 4, no. 2, 2015.

[32] A. L. Berhanu et al., "A review of the applications of Schiff bases as optical chemical sensors," TrAC Trends in Analytical Chemistry, vol. 116, 2019.

[33] F. A. Drobniewski, "Bacillus cereus and related species," Clin. Microbiol. Rev., vol. 6, no. 4, 1993.

[34] P. E. Granum and T. Lindbäck, “Bacillus cereus,” Food Microbiol., 2014.

[35] M. Ehling-Schulz, R. Knutsson, and S. Scherer, “Bacillus cereus,” Genomes of Foodborne and Waterborne Pathogens, 2014.

[36] V. Gupta, J. Kaur, and J. Chander, “An increase in enteric fever cases due to Salmonella Paratyphi A in & around Chandigarh,” Indian Journal of Medical Research, vol. 129, no. 1, 2009.

[37] R. L. Ochiai et al., “Salmonella Paratyphi A Rates, Asia - Volume 11, Number 11—November 2005 - Emerging Infectious Diseases journal - CDC,” Emerg. Infect. Dis., vol. 11, no. 11, 2005.

[38] M. M. Gibani et al., “Homologous and heterologous re-challenge with Salmonella Typhi and Salmonella Paratyphi A in a randomised controlled human infection model,” PLoS Negl. Trop. Dis., vol. 14, no. 10, 2020.

[39] B. Li, Y. Zhao, C. Liu, Z. Chen, and D. Zhou, “Molecular Pathogenesis of Klebsiella Pneumoniae,” Future Microbiol., vol. 9, no. 9, 2014.

[40] J. Yang, K. Zhang, C. Ding, S. Wang, W. Wu, and X. Liu, “Exploring multidrug-resistant Klebsiella pneumoniae antimicrobial resistance mechanisms through whole genome sequencing analysis,” BMC Microbiol., vol. 23, no. 1, 2023.

[41] A. A. Shah, A. S. S. Alwashmi, A. Abalkhail, and A. M. Alkahtani, “Emerging challenges in Klebsiella pneumoniae: Antimicrobial resistance and novel approach,” Microb. Pathog., vol. 202, 2025.

[42] R. Wang, Y. Zhong, X. Gu, J. Yuan, A. F. Saeed, and S. Wang, "The pathogenesis, detection, and prevention of Vibrio parahaemolyticus," Front. Microbiol., vol. 6, 2015.

[43] Y. C. Su and C. Liu, "Vibrio parahaemolyticus: A concern of seafood safety," Food Microbiol., vol. 24, no. 6, 2007.

[44] L. Li, H. Meng, D. Gu, Y. Li, and M. Jia, "Molecular mechanisms of Vibrio parahaemolyticus pathogenesis," Microbiol. Res., vol. 222, no. 1, 2019.

[45] N. Allocati, M. Masulli, M. F. Alexeyev, and C. Di Ilio, "Escherichia coli in Europe: An Overview," International Journal of Environmental Research and Public Health 2013, Vol. 10, Pages 6235-6254, vol. 10, no. 12, 2013.

[46] C. S. Beauchamp and J. N. Sofos, "Diarrheagenic Escherichia coli," Pathogens and Toxins in Food: Challenges and Interventions, 2014.

[47] J. B. Kaper, J. P. Nataro, and H. L. T. Mobley, "Pathogenic Escherichia coli," Nature Reviews Microbiology 2004 2:2, vol. 2, no. 2, 2004.

[48] T. JFOSTER, "Staphylococcus aureus," Molecular Medical Microbiology, 2002.

[49] K. S. Seo and G. A. Bohach, "Staphylococcus aureus," Food Microbiol., 2014.

[50] M. Otto, "Staphylococcus aureus toxins," Curr. Opin. Microbiol., vol. 17, no. 1, 2014.

[51] J.Mohan, Organic Spectroscopy: Principle and Application, 2nd ed. New Delhi: Narosa Publishing House, 2004.

[52] Kemp W, Organic Spectroscopy. London: The Macmillan Press Ltd, 1975.